



# Path Selection and Rate Allocation in Self-Backhauled mmWave Networks

Trung Kien Vu, Chen-Feng Liu, Mehdi Bennis, Merouane Debbah, Matti Latva-Aho

## ► To cite this version:

Trung Kien Vu, Chen-Feng Liu, Mehdi Bennis, Merouane Debbah, Matti Latva-Aho. Path Selection and Rate Allocation in Self-Backhauled mmWave Networks. 2018 IEEE Wireless Communications and Networking Conference (WCNC), Apr 2018, Barcelona, Spain. hal-01962088

**HAL Id: hal-01962088**

**<https://hal-centralesupelec.archives-ouvertes.fr/hal-01962088>**

Submitted on 20 Dec 2018

**HAL** is a multi-disciplinary open access archive for the deposit and dissemination of scientific research documents, whether they are published or not. The documents may come from teaching and research institutions in France or abroad, or from public or private research centers.

L'archive ouverte pluridisciplinaire **HAL**, est destinée au dépôt et à la diffusion de documents scientifiques de niveau recherche, publiés ou non, émanant des établissements d'enseignement et de recherche français ou étrangers, des laboratoires publics ou privés.

# Path Selection and Rate Allocation in Self-Backhauled mmWave Networks

Trung Kien Vu\*, Chen-Feng Liu\*, Mehdi Bennis\*, M erouane Debbah<sup>†</sup>, and Matti Latva-aho\*

\*Centre for Wireless Communications, University of Oulu, Finland

<sup>†</sup>Mathematical and Algorithmic Sciences Lab, Huawei France R&D, Paris, France, and

<sup>†</sup>CentraleSupélec, Universit  Paris-Saclay, Gif-sur-Yvette, France

E-mail: {trungkien.vu, chen-feng.liu, mehdi.bennis, matti.latva-aho}@oulu.fi, merouane.debbah@huawei.com

**Abstract**—We investigate the problem of multi-hop scheduling in self-backhaul mmWave networks, owing to the high path loss of mmWave, multi-hop routes between the macro base station and the intended users via full-duplex small cells need to be carefully selected. This paper addresses the fundamental question: “how to select the best paths and to allocate rates over paths subject to latency constraints with a guaranteed probability?”. To answer this question, we propose a new system design, which factors in channel variations and network dynamics. The problem is cast as a network utility maximization subject to a bounded delay constraint with a guaranteed probability and network stability. The studied problem is decoupled into path/route selection and rate allocation, whereby learning the best paths is done by means of a reinforcement learning algorithm, and the rate allocation is solved by applying the successive convex approximation method. Via numerical results, our approach ensures reliable communication with a guaranteed probability of 99.9999%, and reduces latency by 50.64% and 92.9% as compared to baselines, respectively.

**Index Terms**—Self-backhaul, mmWave communications, multi-hop scheduling, ultra dense small cells, stochastic optimization, non-convex optimization.

## I. INTRODUCTION

To support reliable communication with an over-the-air latency of few milliseconds and extreme throughput, a number of candidate solutions are currently investigated for 5G: 1) higher frequency spectrum, e.g., centimeter and millimeter waves (mmWaves); 2) advanced spectral-efficient techniques, e.g., massive multiple-input multiple-output (MIMO); and 3) ultra-dense self-backhauled small cell deployments [1].

In this paper, we are motivated by the combination of the above techniques, which holds the promise of providing great enhancements of the overall system performance [1], [2]. To do so, an in-band wireless backhauling solution allows to deploy such ultra-dense small cells [2], [3] when massive MIMO and mmWave are combined to provide the wireless backhaul. Although, mmWave frequency bands offer huge bandwidth to meet the exponentially growing traffic demands [3], [4], operating at higher frequency bands experiences high propagation attenuation [4], which requires smart beamforming to achieve highly directional gain [5]. Owing to the short wavelength, mmWave frequency bands allow for packing a massive number of antennas into highly directional beamforming over a short distance as compared to the conventional frequency bands [4]. Besides, mmWave communication requires higher transmit power and is very sensitive to blockage, when transmitting over a long distance [3], [4]. Hence, instead of using a single hop [3], [6], a multi-hop self-backhauling architecture is a promising solution [7], [8]. The authors in [9] studied the multi-hop routing for device-to-device communication, focusing on maximizing the quality for multimedia applications. More importantly, allow-

ing multi-hop transmissions raises a problem of increased delay, which has been ignored. Further, the ultra-dense SC network is mainly operated based on the multi-hop multi-path transmission. Hence, there is a need for fast and efficient multi-hop scheduling with respect to traffic dynamics and channel variance in self-backhauled mmWave networks [7]. To our best knowledge, we are the first to provide a practical and efficient solution for multi-hop multi-path mmWave networks.

**Main contributions:** Considering a multi-hop self-backhauled mmWave network, we propose a new system design to support ultra-reliable and low latency communication (URLLC). In particular, our goal is to maximize a general network utility, subject to a probabilistic delay constraint and network stability. Leveraging the stochastic optimization [10], the studied problem is decoupled into multi-hop path/route selection and rate allocation. We leverage *regret learning* techniques to exploit the benefits of the historical information to aid in selecting the best paths. Second, the rate allocation sub-problem is a non-convex combinatorial program [11], by exploiting the hidden convexity of the problem, we propose an iterative rate allocation based on the second-order cone program (SOCP) in order to obtain a local optimal of the approximated convex problem. The proposed approach answers the following questions: (i) *over which paths the traffic flow should be forwarded?* and (ii) *what is the data rate per flow/sub-flow while ensuring low-latency and ultra-reliability constraints?*

**Related work:** Path selection and multi-path congestion control are well-studied in [12] in which the aggregate utility is increased as more paths are provided. However, splitting data into too many paths leads to increased signaling overhead and makes the traffic congested. Moreover, [12] did *not* consider the problem of providing URLLC. In this paper, we determine the best paths to maximize the network throughput subject to the delay bound violation constraint with a tolerable probability (reliability). A recent work in [13] has studied the multi-hop relaying transmission challenges for mmWave systems, aiming at maximizing the network throughput, while taking account into traffic dynamics and link qualities. In our work, we further address two fundamental questions in multi-hop self-backhauled mmWave networks: (i) *how to select the best paths while taking account into traffic dynamics and link qualities* and (ii) *how to capture the URLLC while maximizing the network utility*. Our previous work [6] studied URLLC-centric mmWave networks for single hop transmission, in this work we extend it to the multi-hop wireless backhaul scenario and study a joint path selection and rate allocation optimization.

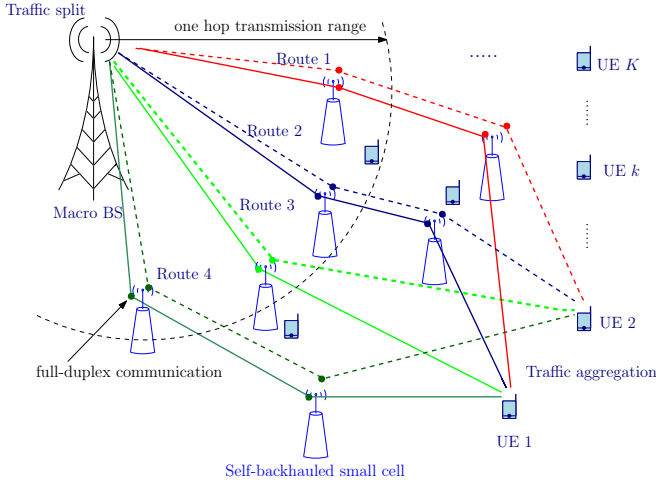


Fig. 1: 5G multi-hop self-backhauled mmWave networks.

## II. SYSTEM MODEL

Let us consider a multi-hop heterogeneous cellular network (HCN) which consists of a macro base station (MBS), a set of  $B$  self-backhauled small cell base stations (SCBSs), and a set  $\mathcal{K}$  of UEs  $K$  single-antenna user equipments (UEs) as shown in Fig. 1. Let  $\mathcal{B} = \{0, 1, \dots, B\}$  denote the set of all BSs in which index 0 refers to the MBS. We consider the downlink transmission in which the traffic is generated from the MBS to UEs via self-backhauled SCBSs and co-channel time-division duplexing (TDD) protocol is considered. The in-band wireless backhaul is used to provide backhaul among base stations (BSs) and a full-duplex transmission protocol is assumed at SCBS with perfect self-interference cancellation [14]. Each BS is equipped with  $N_b$  transmitting antennas and we denote the propagation channel between BS  $b$  and UE  $k$  as  $\mathbf{h}_{(b,k)} = \sqrt{N_b} \Theta_{(b,k)}^{1/2} \tilde{\mathbf{h}}_{(b,k)}$  [3], where  $\Theta_{(b,k)} \in \mathbb{C}^{N_b \times N_b}$  depicts the antenna spatial correlation, and the elements of  $\tilde{\mathbf{h}}_{(b,k)} \in \mathbb{C}^{N_b \times 1}$  are independent and identically distributed (i.i.d.) with zero mean and variance  $1/N_b$ .

The network topology is modeled as a directed graph  $\mathcal{G} = (\mathcal{N}, \mathcal{L})$ , where  $\mathcal{N} = \mathcal{B} \cup \mathcal{K}$  represents the set of nodes including BSs and UEs.  $\mathcal{L} = \{(i, j) | i \in \mathcal{B}, j \in \mathcal{N}\}$  denotes the set of all directional edges  $(i, j)$  in which nodes  $i$  and  $j$  are the transmitter and the receiver, respectively.

We consider a (stochastic) queuing network operating in discrete time  $t \in \mathbb{Z}^+$  [10]. There are  $F$  independent data at the MBS. Each data traffic is destined for one UE, whereas one UE receives multiple data streams, i.e.,  $F \geq K$ . Hereafter, we refer to data traffic as data flow. We use  $\mathcal{F}$  to represent the set of  $F$  data flows. The MBS splits each flow  $f$  into multiple sub-flows which are sent through a set of disjoint paths. The traffic aggregation capability is assumed at the UEs [15].

We assume that there exists  $Z_f$  number of disjoint routes from the MBS to the UE for flow  $f$ . For any disjoint route  $m = \{1, \dots, Z_f\}$ , we denote  $\mathcal{Z}_f^m$  as the route state, which contains all route information such as topology and queue states for every hop. Let  $\mathcal{Z}_f = \{\mathcal{Z}_f^1, \dots, \mathcal{Z}_f^m, \dots, \mathcal{Z}_f^{Z_f}\}$  denote route states observed by flow  $f$ . We use the flow-split indicator vector  $\mathbf{z}_f = (z_f^1, \dots, z_f^{Z_f})$  to denote how the MBS splits flow  $f$ , where  $z_f^m = 1$  means path  $m$  is used to send data for flow  $f$ . Otherwise,  $z_f^m = 0$ . Let  $\mathcal{N}_i^{(o)}$  denote the set of the next hops from node  $i$  via a directional edge. We denote the next hop of flow  $f$  from BS  $b$  as  $b_f^{(o)}$ .

In addition,  $\mathbf{h} = (\mathbf{h}_{(i,j)} | (i, j) \in \mathcal{L})$  consists of the channel propagations and we denote  $p_{(i,j)}^f$  as the transmit

power of node  $i$  assigned to node  $j$  for flow  $f$ , such that  $\sum_{f \in \mathcal{F}} \sum_{j \in \mathcal{N}_i^{(o)}} p_{(i,j)}^f \leq P_i^{\max}$ , where  $P_i^{\max}$  is the maximum transmit power of node  $i$ . We have the power constraint as

$$\mathcal{P} = \left\{ p_{(i,j)}^f \geq 0, i, j \in \mathcal{N}, \left| \sum_{f \in \mathcal{F}} \sum_{j \in \mathcal{N}_i^{(o)}} p_{(i,j)}^f \leq P_i^{\max} \right. \right\}. \quad (1)$$

Vector  $\mathbf{p} = (p_{(i,j)}^f | \forall i, j \in \mathcal{N}, \forall f \in \mathcal{F})$  denotes the transmit power over all flows. Therefore, for a given channel state and transmit power, the data rate in edge  $(i, j)$  over flow  $f$  can be posted as a function of channel state and transmit power, i.e.,  $R_{(i,j)}^f(\mathbf{h}, \mathbf{p})$ , such that  $\sum_{f \in \mathcal{F}} R_{(i,j)}^f = R_{(i,j)}$ . We denote  $\mathbf{R} = (R_{(i,j)}^f | \forall i, j \in \mathcal{N}, \forall f \in \mathcal{F})$  as a vector of data rates over all flows.

Let  $Q_b^f(t)$  denote the queue length<sup>1</sup> at BS  $b$  at time slot  $t$  for flow  $f$ . The queue length evolution at the MBS  $b = 0$  is

$$Q_b^f(t+1) = \left[ Q_b^f(t) - \sum_{m=1, b_f^{(o)} \in \mathcal{Z}_f^m} z_f^m R_{(b, b_f^{(o)})}^f(t), 0 \right]^+ + \mu^f(t). \quad (2)$$

where  $\mu^f(t)$  is the data arrival at the MBS during slot  $t$ , which is independent and identical distributed (i.i.d.) over time with a mean value  $\bar{\mu}^f$ . Due to the disjoint paths, the incoming rate at the SCBS is either from one SCBS or the MBS, which is denoted as  $b^{(l)}$ . The queue evolution at the SCBS  $b = \{1, \dots, B\}$  is given by

$$Q_b^f(t+1) \leq \left[ Q_b^f(t) - R_{(b, b_f^{(o)})}^f(t), 0 \right]^+ + R_{(b^{(l)}, b)}^f(t). \quad (3)$$

## III. PROBLEM FORMULATION

Assume that the MBS determines routes to split data flow  $f$  with a given probability distribution, i.e.,  $\pi_f = (\pi_f^1, \dots, \pi_f^{Z_f} | \pi_f^m = \Pr(z_f = z_f^m))$ . Here,  $\pi_f$  is the probability mass function (PMF) of the flow-split vector, i.e.,  $\sum_{m=1}^{Z_f} \Pr(z_f^m) = 1$ . We denote  $\pi = \{\pi_1, \dots, \pi_f, \dots, \pi_F\} \in \Pi$  as the global probability distribution of all flow-split vectors in which  $\Pi$  is the set of all possible global PMFs. Let  $\bar{x}_0^f$  denote the achievable average rate of flow  $f$ , where  $\bar{x}_0^f \triangleq \lim_{t \rightarrow \infty} \frac{1}{t} \sum_{\tau=1}^t x_0^f(\tau)$  and  $x_0^f(\tau) = \sum_{m=1, b_f^{(o)} \in \mathcal{Z}_f^m} \mathbb{E}[z_f^m R_{(b, b_f^{(o)})}^f(\tau)] | b = 0$ . We assume that the achievable rate is bounded, i.e.,

$$0 \leq x_0^f(t) \leq a_{max}^f, \quad (4)$$

where  $a_{max}^f$  is the maximum achievable rate of flow  $f$  at every time  $t$ . Vector  $\bar{\mathbf{x}} = (\bar{x}_0^1, \dots, \bar{x}_0^F)$  denotes the time average of rates over all flows. Let  $\mathcal{R}$  denote the rate region, which is defined as the convex hull of the average rates, i.e.,  $\bar{\mathbf{x}} \in \mathcal{R}$ .

We define  $U_0$  as a network utility function, i.e.,  $U_0(\bar{\mathbf{x}}) = \sum_{f \in \mathcal{F}} U(\bar{x}_0^f)$ . Here,  $U(\cdot)$  is assumed to be a twice differentiable, concave, and increasing  $L$ -Lipschitz function for all  $\bar{\mathbf{x}} \geq 0$ . According to Little's law [16], the queuing delay is defined as the ratio of the queue length to the average arrival rate. By taking into account the probabilistic delay constraints for each flow/subflow, the following network utility maximization (NUM) is formulated as:

<sup>1</sup>The queues at the UEs are assumed to be empty and to be removed completely from network.

$$\text{OP: } \max_{\pi, \mathbf{x}, \mathbf{p}} U_0(\bar{\mathbf{x}}) \quad (5a)$$

$$\text{subject to } \Pr\left(\frac{Q_b^f(t)}{\bar{\mu}_f} \geq \beta\right) \leq \epsilon, \forall t, f \in \mathcal{F}, b \in \mathcal{B}, \quad (5b)$$

$$\lim_{t \rightarrow \infty} \frac{\mathbb{E}[|Q_b^f|]}{t} = 0, \forall f \in \mathcal{F}, \forall b \in \mathcal{B}, \quad (5c)$$

$$\mathbf{x}(t) \in \mathcal{R}, \quad (5d)$$

$$\boldsymbol{\pi} \in \Pi, \quad (5e)$$

and (1), (4),

where  $\Pr(\cdot)$  denotes the probability operator,  $\beta$  reflects the maximum allowed delay requirement for UEs, and  $\epsilon \ll 1$  is the target probability for reliable communication. The probabilistic delay constraint (5b) implies the probability that the delay for each flow at node  $b$  is greater than  $\beta$  is very small, which captures the constraints of ultra-low latency and reliable communication. It is also used to avoid congestion for each flow  $f$  at any point (BS) in the network, if the queue length is greater than  $\beta \bar{\mu}^f$ . More importantly, (5b) forces the transmission of all BSs, and (5c) maintains network stability.

The above problem has a non-linear probabilistic constraint (5b), which cannot be solved directly. Hence, we replace the non-linear constraint (5b) with a linear deterministic equivalent by applying Markov's inequality [17]. In Markov's inequality, we have  $\Pr(X \geq a) \leq \mathbb{E}[X]/a$  for a non-negative random variable  $X$  and  $a > 0$ . Thus, we relax (5b) as

$$\mathbb{E}[Q_b^f(t)] \leq \bar{\mu}^f \epsilon \beta. \quad (6)$$

Assuming that  $\mu^f(t)$  follows a Poisson arrival process [17], we derive the expected queue length in (2) for  $b = 0$  as

$$\mathbb{E}[Q_b^f(t)] = t\bar{\mu}^f - \sum_{\tau=1}^t \sum_{m=1, b_f^{(\circ)} \in \mathcal{Z}_f^m} \pi_f^m z_f^m R_{(b, b_f^{(\circ)})}^f(\tau), \quad (7)$$

and the expected queue length in (3), for each SCBS, i.e.,

$$\mathbb{E}[Q_b^f(t)] = \sum_{\tau=1}^t \sum_m \pi_f^m z_f^m \left( R_{(b^{(\circ)}, b)}^f(\tau) - R_{(b, b_f^{(\circ)})}^f(\tau) \right). \quad (8)$$

Subsequently, combining the URLLC constraint (6) and (7), we obtain, for the MBS  $b = 0$ ,

$$\begin{aligned} & \bar{\mu}^f(t - \epsilon\beta) - \sum_{\tau=1}^{t-1} \sum_{m=1, b_f^{(\circ)} \in \mathcal{Z}_f^m} \pi_f^m z_f^m R_{(b, b_f^{(\circ)})}^f(\tau) \\ & \leq \sum_{m=1, b_f^{(\circ)} \in \mathcal{Z}_f^m} \pi_f^m z_f^m R_{(b, b_f^{(\circ)})}^f(t). \end{aligned} \quad (9)$$

Similarly, for each SCBS  $b = \{1, \dots, B\}$ , we have

$$\begin{aligned} & -\bar{\mu}^f \epsilon \beta + \sum_{\tau=1}^{t-1} \sum_m \pi_f^m z_f^m \left( R_{(b^{(\circ)}, b)}^f(\tau) - R_{(b, b_f^{(\circ)})}^f(\tau) \right) \\ & \leq \sum_m \pi_f^m z_f^m \left( R_{(b, b_f^{(\circ)})}^f(t) - R_{(b^{(\circ)}, b)}^f(t) \right), \end{aligned} \quad (10)$$

by combining (6) and (8). With the aid of the above derivations, we consider (9) and (10) instead of (5b) in the original problem (5). In practice, since the statistical information of all candidate paths to decide  $\pi_f, \forall f \in \mathcal{F}$ , is not available beforehand, that would be very challenging when solving (5). One solution is that paths are randomly assigned to each flow

which does not guarantee optimality, whereas applying the high-complexity exhaustive search is not practical. Therefore, in this work, we propose a low-complexity approach by invoking the tools from Lyapunov stochastic optimization which achieves the optimal performance without requiring the statistical information beforehand.

#### IV. PROPOSED ALGORITHM

Let us start by rewriting (5) equivalently as [10]

$$\text{RP: } \max_{\bar{\boldsymbol{\varphi}}, \boldsymbol{\pi}, \mathbf{p}} U_0(\bar{\boldsymbol{\varphi}}) \quad (11a)$$

$$\text{subject to } \bar{\varphi}_0^f - \bar{x}_0^f \leq 0, \forall f \in \mathcal{F}, \quad (11b)$$

(1), (4), (5c), (5e), (9), (10),

where the new constraint (11b) is introduced to replace the rate constraint (5d) with new auxiliary variables  $\boldsymbol{\varphi} = (\varphi_0^1, \dots, \varphi_0^F)$ . In (11b),  $\bar{\boldsymbol{\varphi}} \triangleq \lim_{t \rightarrow \infty} \frac{1}{t} \sum_{\tau=1}^t \mathbb{E}[|\boldsymbol{\varphi}(\tau)|]$ . In order to ensure the inequality constraint (11b), we introduce a virtual queue vector  $Y_0^f(t)$ , which is given by

$$Y_0^f(t+1) = \left[ Y_0^f(t) + \varphi_0^f(t) - x_0^f(t) \right]^+, \forall f \in \mathcal{F}. \quad (12)$$

Then, we write the conditional Lyapunov drift-plus-penalty for slot  $t$  as

$$\Delta(\boldsymbol{\Sigma}(t)) = \mathbb{E}[L(\boldsymbol{\Sigma}(t+1)) - L(\boldsymbol{\Sigma}(t)) | \boldsymbol{\Sigma}(t)] - \nu U_0(\bar{\boldsymbol{\varphi}}), \quad (13)$$

where  $L(\boldsymbol{\Sigma}(t)) \triangleq \frac{1}{2} \left[ \sum_{f=1}^F \sum_{b=0}^B Q_b^f(t)^2 + \sum_{f=1}^F Y_0^f(t)^2 \right]$  is the quadratic Lyapunov function of the queue backlogs  $\boldsymbol{\Sigma}(t) = (\mathbf{Q}(t), \mathbf{Y}(t))$  [10]. Here,  $\nu$  is a control parameter, which is chosen to trade off utility optimality and queue length. Note that the stability of  $\boldsymbol{\Sigma}(t)$  assures that the constraints of problem (5c) and (11b) are held. Subsequently, following the straightforward calculations of the Lyapunov optimization which are omitted here for space, we obtain

$$\begin{aligned} (13) & \leq \sum_{f=1}^F \sum_{b=1}^B \sum_m \pi_f^m z_f^m Q_b^f \left( R_{(b^{(\circ)}, b)}^f - R_{(b, b_f^{(\circ)})}^f \right) \\ & - \sum_{f=1}^F \sum_{m=1, b_f^{(\circ)} \in \mathcal{Z}_f^m} \pi_f^m z_f^m Q_b^f R_{(b, b_f^{(\circ)})}^f \Big|_{b=0} \quad (14) \\ & + \sum_{f=1}^F \left[ Y_0^f \varphi_0^f - \nu U(\varphi_0^f) - Y_0^f x_0^f \right] + \Psi. \end{aligned}$$

Due to space limitation, we omit the details of the constant value  $\Psi$ , which does not influence the system performance [10]. The solution to (11) can be obtained by minimizing the upper bound in (14), in which we have three decoupled sub-problems as follows: The flow-split vector and the probability distribution are determined by

$$\begin{aligned} \text{SP1: } & \min_{\boldsymbol{\pi}, \mathbf{z}} \sum_{f=1}^F \Xi_f \\ & \text{subject to } (5e), \end{aligned}$$

where

$$\begin{aligned} \Xi_f & = \sum_{b=1}^B \sum_m \pi_f^m z_f^m Q_b^f \left( R_{(b^{(\circ)}, b)}^f - R_{(b, b_f^{(\circ)})}^f \right) \\ & - \sum_{m=1, b_f^{(\circ)} \in \mathcal{Z}_f^m} \pi_f^m z_f^m Q_b^f R_{(b, b_f^{(\circ)})}^f \Big|_{b=0}. \end{aligned}$$

Then, we select the optimal auxiliary variables by solving the following convex optimization problem

$$\begin{aligned} \text{SP2: } \min_{\varphi|\mathbf{z}} \quad & \sum_{f=1}^F \left[ Y_0^f \varphi_0^f - \nu U(\varphi_0^f) \right] \\ \text{subject to} \quad & \varphi_0^f(t) \geq 0, \forall f \in \mathcal{F}. \end{aligned}$$

Let  $\varphi_0^{f*}$  be the optimal solution obtained by the first order derivative of the objective function of SP2. Assuming a logarithmic utility function, we have  $\varphi_0^{f*}(t) = \max\left\{\frac{\nu}{Y_0^f}, 0\right\}$ . Finally, the rate allocation is done by assigning transmit power, which is obtained by

$$\begin{aligned} \text{SP3: } \min_{\mathbf{x}, \mathbf{p}|\mathbf{z}} \quad & \sum_{f=1}^F -Y_0^f x_0^f \\ \text{subject to} \quad & (1), (4), (9), (10). \end{aligned}$$

### A. Route Selection

To select the optimal routes in SP1, we leverage regret reinforcement learning which exploits the historical system information such as queue state and channel state [18]. The intuition behind this approach is that the regret learning method results in maximizing the long-term utility for each flow, by leveraging stochastic optimization [10], which allows to design the optimal utility-delay trade-off.

We denote  $u_f^m = u_f(z_f^m, \mathbf{z}_f^{-m})$  as an utility function of flow  $f$  when using path  $m$ . The vector  $\mathbf{z}_f^{-m}$  denotes the flow-split vector excluding path  $m$ . The MBS probably chooses more than one path to deliver data, from SP1, the utility gain of flow  $f$  is

$$u_f = \sum_m u_f^m = -\Xi_f.$$

To exploit the historical information, the MBS determines a flow-split vector for each flow  $f$  from  $\mathcal{Z}_f$  based on the PMF from the previous stage  $t-1$ , i.e.,

$$\pi_f(t-1) = \left( \pi_f^1(t-1), \dots, \pi_f^m(t-1) \dots, \pi_f^{Z_f}(t-1) \right). \quad (15)$$

Here, we define  $\mathbf{r}_f(t) = (r_f^1(t), \dots, r_f^m(t) \dots, r_f^{Z_f}(t))$  as a regret vector of determining flow-split vector for flow  $f$ . The MBS tends to determine the flow-split vector with highest regret in which the mixed-strategy probability is given as

$$\pi_f^m(t) = \frac{\left[ r_f^m(t) \right]^+}{\sum_{m' \in \mathcal{Z}_f} \left[ r_f^{m'}(t) \right]^+}. \quad (16)$$

We introduce the Boltzmann-Gibbs (BG) distribution,  $\beta_f^m(\tilde{\mathbf{r}}_f(t))$  to capture the exploitation and exploration for efficient learning, given by

$$\beta_f^m(\tilde{\mathbf{r}}_f(t)) = \underset{\pi_f \in \Pi}{\operatorname{argmax}} \sum_{m \in \mathcal{Z}_f} \left[ \pi_f^m(t) \tilde{r}_f^m(t) - \kappa_f \pi_f^m(t) \ln(\pi_f^m(t)) \right], \quad (17)$$

where  $\tilde{\mathbf{r}}_f(t) = (\tilde{r}_f^1(t), \dots, \tilde{r}_f^m(t) \dots, \tilde{r}_f^{Z_f}(t))$  is the estimated regret vector of flow  $f$ , and the trade-off factor  $\kappa_f$  is used to balance between exploration and exploitation. If  $\kappa_b$  is small, the SC selects  $\mathbf{z}_b$  with highest payoff. For  $\kappa_b \rightarrow \infty$  all decisions have equal chance.

For given set of  $\tilde{\mathbf{r}}_f(t)$  and  $\kappa_f$ , we solve (17) to find the probability distribution in which the solution determining the disjoint routes for each flow  $f$  is given as

$$\beta_f^m(\tilde{\mathbf{r}}_f(t)) = \frac{\exp\left(\frac{1}{\kappa_f} \left[ \tilde{r}_f^m(t) \right]^+\right)}{\sum_{m' \in \mathcal{Z}_f} \exp\left(\frac{1}{\kappa_f} \left[ \tilde{r}_f^{m'}(t) \right]^+\right)}. \quad (18)$$

We denote  $\tilde{u}(t)$  as the estimated utility of flow  $f$  at time instant  $t$  with action  $\mathbf{z}_f$ , i.e.,  $\tilde{\mathbf{u}}_f(t) = (\tilde{u}_f^1(t), \dots, \tilde{u}_f^m(t) \dots, \tilde{u}_f^{Z_f}(t))$ . In addition,  $\hat{u}_f(t)$  denotes the utility observed by flow  $f$ , i.e.,  $\hat{u}_f(t) = u_f(t-1)$ . Finally, we propose the learning mechanism at each time instant  $t$  as follows.

**Learning procedure:** The estimates of the utility, regret, and probability distribution functions are performed, and are updated for all actions as follows:

$$\begin{cases} \tilde{u}_f^m(t) = \tilde{u}_f^m(t-1) + \xi_f(t) \mathbb{I}_{\{\mathbf{z}_f = \mathbf{z}_f^m\}} \left( \hat{u}_f(t) - \tilde{u}_f^m(t-1) \right), \\ \tilde{r}_f^m(t) = \tilde{r}_f^m(t-1) + \gamma_f(t) \left( \tilde{u}_f^m(t) - \hat{u}_f(t) - \tilde{r}_f^m(t-1) \right), \\ \pi_f^m(t) = \pi_f^m(t-1) + \iota_f(t) \left( \beta_f^m(\tilde{\mathbf{r}}_f(t)) - \pi_f^m(t-1) \right), \end{cases} \quad (19)$$

Here,  $\xi_f(t)$ ,  $\gamma_f(t)$ , and  $\iota_f(t)$  are the learning rates which are chosen to satisfy the convergence properties (please see [18] for more details and convergence proof). Based on the probability distribution as per (19), the MBS determines the flow-split vector for each flow  $f$  as defined in Section III. Note that the learning-aided route selection<sup>2</sup> is performed in a long-term period to ensure that the routes do not suddenly change such that the SCBSs have enough time to release traffic from the queues.

### B. Rate Allocation

Consider  $R_{(i,j)}^f = \log(1 + p_{(i,j)}^f |g_{(i,j)}(\mathbf{h})|^2)$  as the transmission rate, where the effective channel gain<sup>3</sup> for mmWave channels can be modeled as  $g_{(i,j)}(\mathbf{h}) = \frac{\tilde{g}_{(i,j)}(\mathbf{h})}{1 + I^{\max}}$  [5]. Here, under the noise-limited regime of mmWave channels  $\tilde{g}_{(i,j)}(\mathbf{h})$  and  $I^{\max}$  denote the normalized channel gain and the maximum interference, respectively [3]. Denoting the left hand side (LHS) of (9) and (10) as  $D_b^f$  for simplicity, the optimal values of flow control  $\mathbf{x}$  and transmit power  $\mathbf{p}$  are found by minimizing

$$\min_{\mathbf{x}, \mathbf{p}|\mathbf{z}} \sum_{f=1}^F -Y_0^f x_0^f \quad (20a)$$

$$\text{subject to } 1 + p_{(0,0^{\circ})}^f |g_{(0,0^{\circ})}|^2 \geq e^{x_0^f}, \forall f \in \mathcal{F}, \quad (20b)$$

$$\frac{1 + p_{(b,b_f^{\circ})}^f |g_{(b,b_f^{\circ})}|^2}{1 + p_{(b^{(1)},b)}^f |g_{(b^{(1)},b)}|^2} \geq e^{D_b^f}, \forall b \in \mathcal{S}^f, f \in \mathcal{F}, \quad (20c)$$

$$\sum_{f \in \mathcal{F}} p_{(b,b_f^{\circ})}^f \leq P_b^{\max}, \forall b \in \mathcal{B}, \forall f \in \mathcal{F}. \quad (20d)$$

The constraint (20c) is non-convex, and the LHS of (20c) is an affine-over-affine function, which is jointly convex w.r.t the corresponding variables [19], [11]. By exploiting the hidden convexity of the problem, we propose an iterative rate allocation based on the successive convex approximation

<sup>2</sup>Moreover, the routes are decided before transmission, which helps designing smart beamforming and beam-alignment to achieve higher directional gain, while mitigating interference.

<sup>3</sup>The effective channel gain captures the path loss, channel variations, and interference penalty (Here, the impact of interference is considered small due to highly directional beamforming and high pathloss for interfered signals at mmWave frequency band.).

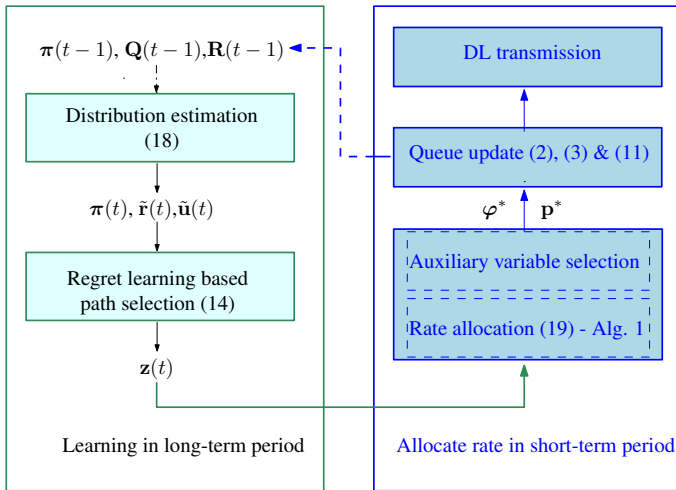


Fig. 2: Information flow diagram of the learning-aided path selection and rate allocation.

method. In this regard, we introduce the slack variable  $y$  to (20c) and rewrite it as

$$\frac{2 + p_{(b,b_f^{(o)})}^f |g_{(b,b_f^{(o)})}|^2}{2} \geq \sqrt{y^2 + \left( \frac{p_{(b,b_f^{(o)})}^f |g_{(b,b_f^{(o)})}|^2}{2} \right)^2}, \quad (21)$$

$$\frac{y^2}{1 + p_{(b^{(l)},b)}^f |g_{(b^{(l)},b)}|^2} \geq e^{D_b^f}. \quad (22)$$

Here, the constraint (21) holds a form of the second-order cone inequalities [11], while the LHS of constraint (22) is a quadratic-over-affine function which is iteratively replaced by the first order to achieve a convex approximation as follow

$$\frac{2yy^{(l)}}{1 + p_{(b^{(l)},b)}^f |g_{(b^{(l)},b)}|^2} - \frac{y^{(l)2} \left( 1 + p_{(b^{(l)},b)}^f |g_{(b^{(l)},b)}|^2 \right)}{\left( 1 + p_{(b^{(l)},b)}^f |g_{(b^{(l)},b)}|^2 \right)^2}. \quad (23)$$

Here, the superscript  $l$  denotes the  $l$ th iteration. Hence, we iteratively solve the approximated convex problem of (20) as **Algorithm 1** in which the approximated problem is given as

$$\begin{aligned} \min_{\mathbf{x}, \mathbf{p} | \mathbf{z}} \quad & \sum_{f=1}^F -Y_0^f x_0^f \\ \text{subject to} \quad & (20b), (4), (20d), (21), (23). \end{aligned} \quad (24)$$

Finally, the information flow diagram of the learning-aided path selection and rate allocation approach is shown in Fig. 2, where the rate allocation is executed in a short-term period.

---

#### Algorithm 1 Iterative rate allocation

---

Initialization: set  $l = 0$  and generate initial points  $y^{(l)}$ .

**repeat**

Solve (24) with  $y^{(l)}$  to get the optimal value  $y^{(l)*}$ .

Update  $y^{(l+1)} := y^{(l)*}$ ;  $l := l + 1$ .

**until** Convergence

---

## V. NUMERICAL RESULTS

In this section, we provide numerical results by assuming two flows from the MBS to two UEs, while the number

of available paths for each flow is four [12]. The MBS determines two best routes from four most popular routes<sup>4</sup>. Each route contains one or two relays, the one-hop distance is varying from 50 to 100 meters. The maximum transmit power of MBS and each SC are 43 dBm and 30 dBm, respectively. The SC antenna gain is 5 dBi and the number of antennas at each BS is  $N_b = 8$ . We assume that the traffic flow is divided equally into two subflows, the arrival rate for each sub-flow is varying from 2 to 5 Gbps. The path loss is modeled as a distance-based path loss with the line-of-sight (LOS) model<sup>5</sup> for urban environments at 28 GHz with 1 GHz of bandwidth [20]. The maximum delay requirement  $\beta$  and the target reliability probability  $\epsilon$  are set to be 10 ms and 5%, respectively [6]. For the learning algorithm, the Boltzmann temperature (trade-off factor)  $\kappa_f$  is set to 5, while the learning rates  $\xi_f(t)$ ,  $\gamma_f(t)$ , and  $\iota_f(t)$  are set to  $\frac{1}{(t+1)^{0.5}}$ ,  $\frac{1}{(t+1)^{0.55}}$ , and  $\frac{1}{(t+1)^{0.6}}$ , respectively [18].

Furthermore, we compare our proposed scheme with the following baselines:

- **Baseline 1** considers a general NUM framework [10] with the best path learning function [18].
- **Baseline 2** considers a general NUM framework [10] and a random path section scheme, subject to (5b).
- **Baseline 3** considers a general NUM framework [10] and a random path section scheme.
- **Single hop** scheme: The MBS delivers data to UEs over one single hop at long distance in which the probability of LOS communication is low, and then the blockage needs to be taken into account [20].

In Fig. 3, we report the average one-hop delay<sup>6</sup> versus the mean arrival rates  $\bar{\mu}$ . As we increase  $\bar{\mu}$ , **baseline 3** violates the latency constraints, whereas our proposed algorithm outperforms the other **baselines**. The average one-hop delay of **baseline 1** with learning outperforms **baselines 2** and **3**, whereas our proposed scheme reduces latency by 50.64%, 81.32% and 92.9% as compared to **baselines 1**, **2**, and **3**, respectively, when  $\lambda = 4.5$  Gbps. When  $\lambda = 5$  Gbps, the average delay of all **baselines** increases, violating the delay requirement of 10ms, while our proposed scheme is robust to the latency requirement. Moreover, for throughput comparison, we observe that as  $\lambda = 4.5$  Gbps, our proposed algorithm is able to deliver 4.4874 Gbps of average network throughput per each subflow, while the **baselines 1**, **2**, and **3** deliver 4.4759, 4.4682, and 4.3866 Gbps, respectively. Here, the **single hop** scheme only delivers 3.55 Gbps due to the blockage, which resulting in large delay.

In Fig. 4, we report the tail distribution (complementary cumulative distribution function (CCDF)) of latency to show-case how often the system achieves a delay greater than the target delay levels. In contrast to the average delay, the tail distribution is an important metric to reflect the URLLC characteristic. For instance, at  $\lambda = 4.5$  Gbps, by imposing the probabilistic latency constraint, our proposed approach ensures reliable communication with better guaranteed probability, i.e,  $\Pr(\text{Delay} > 10\text{ms}) < 10^{-6}$ . In contrast, **baseline**

<sup>4</sup>As studied in [12], it suffices for a flow to maintain at least two paths provided that it repeatedly selects new paths at random and replaces if the latter provides higher throughput.

<sup>5</sup>The probability of LOS communication is assumed to be high for one-hop transmission, while the blockage channel is modeled for the baseline with single-hop scheme.

<sup>6</sup>The average end-to-end delay can be defined as the sum of the average one-hop delay of all hops.

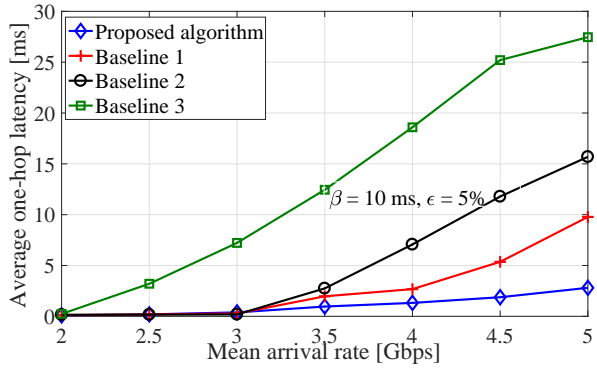


Fig. 3: Average one-hop delay versus mean arrival rates,  $\epsilon = 5\%$ ,  $\beta = 10$  ms,  $\kappa = 5$ .

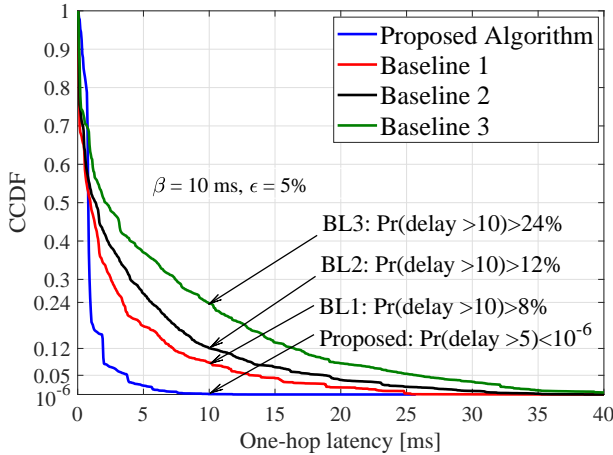


Fig. 4: CCDF of the one-hop latency,  $\bar{\mu} = 4.5$  Gbps,  $\epsilon = 5\%$ ,  $\beta = 10$  ms,  $\kappa = 5$ .

1 with learning violates the latency constraint with high probability, where  $\Pr(\text{Delay} > 10\text{ms}) = 8\%$  and  $\Pr(\text{Delay} > 25\text{ms}) < 10^{-6}$ , while the performance of **baselines 2 and 3** gets worse.

In Fig. 5, we report the tail distribution of one-hop latency versus the guaranteed probability  $\epsilon$ . By varying  $\epsilon$  from 5% to 15%, the system achieves a delay greater than the target delay levels with higher probability. As can be seen in Fig. 5, the probability that the system achieves a delay greater than 4 ms increases when increasing  $\epsilon$ .

## VI. CONCLUSION

In this paper, we have proposed a multi-hop scheduling to ensure URLLC by incorporating the probabilistic latency constraint in 5G self-backhauled mmWave networks. In particular, the problem is modeled as a network utility maximization subject to a probabilistic latency constraints with a guaranteed probability and queue stability. We have proposed a dynamic approach, which adapts to channel variations and system dynamics. We leverage the stochastic optimization to decouple the studied problem into path selection and rate allocation. Numerical results show that our proposed framework reduces latency by 50.64% and 92.9% as compared to **baselines** with and without learning, respectively.

## ACKNOWLEDGMENT

The authors would like to thank the Finnish Funding Tekes, Nokia, Huawei, MediaTek, Keysight, Bittium and Kyynel for project funding. The Academy of Finland, the Nokia Foundation, and the Riitta and Jorma J Takanen Foundation SR are also acknowledged.

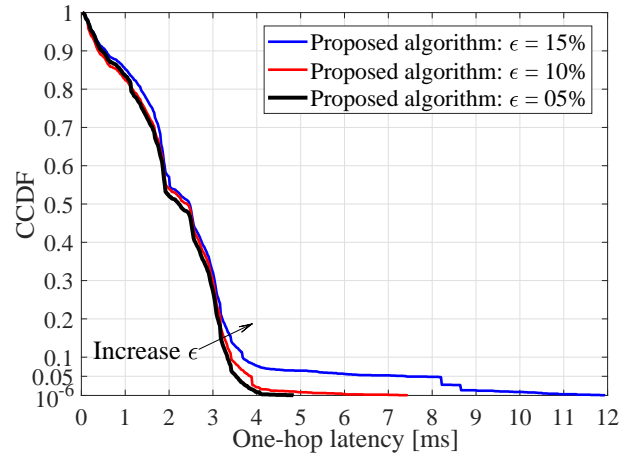


Fig. 5: CCDF of the one-hop latency versus the guaranteed probability  $\epsilon$ ,  $\beta = 10$  ms,  $\kappa = 5$ , and  $\bar{\mu} = 4.5$  Gbps.

## REFERENCES

- [1] J. G. Andrews et al., “What Will 5G Be?” *IEEE Journal on Selected Areas in Communications*, vol. 32, no. 6, pp. 1065–1082, June 2014.
- [2] A. Anpalagan, M. Bennis, and R. Vannithamby, *Design and Deployment of Small Cell Networks*. Cambridge University Press, 2015.
- [3] T. K. Vu et al., “Joint load balancing and interference mitigation in 5g heterogeneous networks,” *IEEE Transactions on Wireless Communications*, vol. 16, no. 9, pp. 6032–6046, Sep. 2017.
- [4] T. S. Rappaport et al., “Millimeter wave mobile communications for 5G cellular: It will work!” *IEEE Access*, vol. 1, pp. 335–349, 2013.
- [5] S. Hur et al., “Millimeter wave beamforming for wireless backhaul and access in small cell networks,” *IEEE Trans. Commun.*, vol. 61, no. 10, pp. 4391–4403, Oct. 2013.
- [6] T. K. Vu et al., “Ultra-reliable and low latency communication in mmwave-enabled massive mimo networks,” *IEEE Communications Letters*, vol. 21, no. 9, pp. 2041–2044, Sep. 2017.
- [7] Qualcomm Technologies, Inc., “Leading the path towards 5G with LTE Advanced Pro,” White Paper, 2016.
- [8] S. Singh, F. Ziliotto, U. Madhow, E. Belding, and M. Rodwell, “Blockage and directivity in 60 GHz wireless personal area networks: From cross-layer model to multihop MAC design,” *IEEE Journal on Selected Areas in Communications*, vol. 27, no. 8, 2009.
- [9] N. Eshraghi et al., “Millimeter-wave device-to-device multi-hop routing for multimedia applications,” in *Proc. IEEE Int. Conf. Commun.*, Kuala Lumpur, Malaysia, May 2016, pp. 1–6.
- [10] M. J. Neely, “Stochastic network optimization with application to communication and queueing systems,” *Synthesis Lectures on Communication Networks*, vol. 3, no. 1, pp. 1–211, 2010.
- [11] S. Boyd and L. Vandenberghe, *Convex optimization*. Cambridge university press, 2004.
- [12] P. Key et al., “Path selection and multipath congestion control,” in *Proc. the 26th IEEE Int. Conf. on Computer Communications (INFOCOM)*. Barcelona, Spain: IEEE, 2007, pp. 143–151.
- [13] B. Sahoo, C.-H. Yao, and H.-Y. Wei, “Millimeter-wave multi-hop wireless backhauling for 5g cellular networks,” in *Proc. IEEE 85th Vehicular Technology Conf.*, Sydney, Australia, June 2017, pp. 1–6.
- [14] T. K. Vu, M. Bennis, S. Samarakoon, M. Debbah, and M. Latvaaho, “Joint in-band backhauling and interference mitigation in 5G heterogeneous networks,” in *Proc. 22th European Wireless Conf.*, Oulu, Finland, May 2016, pp. 1–6.
- [15] A. Zakrzewska et al., “Dual connectivity in LTE HetNets with split control-and user-plane,” in *Proc. IEEE Global Commun. Conf. Workshops*, Atlanta, GA, USA, Dec. 2013, pp. 391–396.
- [16] J. D. Little and S. C. Graves, “Little’s law,” in *Building intuition*. Springer, 2008, pp. 81–100.
- [17] A. Mukherjee, “Queue-aware dynamic on/off switching of small cells in dense heterogeneous networks,” in *Proc. IEEE Global Commun. Conf. Workshops*, Atlanta, GA, USA, Dec. 2013, pp. 182–187.
- [18] M. Bennis, S. M. Perlaza, and M. Debbah, “Learning coarse correlated equilibria in two-tier wireless networks,” in *Proc. IEEE Int. Conf. Commun.*, Ottawa, ON, Canada, Jun. 2012, pp. 1592–1596.
- [19] K. G. Nguyen et al., “Achieving energy efficiency fairness in multicell MISO downlink,” *IEEE Communications Letters*, vol. 19, no. 8, pp. 1426–1429, 2015.
- [20] M. R. Akdeniz, Y. Liu, M. K. Samimi, S. Sun, S. Rangan, T. S. Rappaport, and E. Erkip, “Millimeter wave channel modeling and cellular capacity evaluation,” *IEEE J. Sel. Areas Commun.*, vol. 32, no. 6, pp. 1164–1179, Jun. 2014.